

A Model Study of the Response of Mesospheric Ozone to Short-Term Solar Ultraviolet Flux Variations

M. E. SUMMERS,¹ D. F. STROBEL,^{2,3} R. M. BEVILACQUA,¹ XUN ZHU,²
M. T. DELAND,⁴ M. ALLEN,⁵ AND G. M. KEATING⁶

A one-dimensional photochemical model and a time-dependent heat equation which incorporates non-local thermodynamic equilibrium (non-LTE) IR radiative transfer are used to study the response of mesospheric ozone concentration to short-term solar UV flux variations. We compare our model results with the observed ozone response obtained from a statistical analysis of Solar Mesosphere Explorer (SME) data (Keating et al., 1987). Our model with sinusoidal 27-day-period forcing of mesospheric chemistry by solar ultraviolet flux, when combined with temperature-chemistry feedback, time-dependent atmospheric temperature effects, and low eddy mixing rates, reproduces the major characteristics of the observed ozone response but not the observed temperature response. Below 60 km the calculated response shows a strong dependence on the magnitude of the assumed flux modulation in the Hartley region of the spectrum. A comparison of the model O₃ response with the SME observations suggests that there is negligible 27-day variation of solar flux longward of 2400 Å, in agreement with Lean (1987). The magnitude of the computed ozone response to increased solar UV flux in the upper mesosphere (above 70 km) is strongly coupled to the water vapor abundance through the HO_x catalytic cycle that removes ozone. Our model predicts the essential aspects of the observed ozone response only when the water vapor mixing ratio and vertical eddy diffusion coefficient are a factor of 5 below observed and inferred mid-latitude values. But then the model results are in almost complete disagreement with the observed temperature amplitude and phase lag. Calculations performed with imposition of the temperature response observed by Keating et al. (1987) produces an ozone response in the middle mesosphere in severe conflict with observations, suggesting a need for better mesospheric and solar data and further modeling efforts to determine the role of dynamics in the mesospheric ozone and temperature response to solar UV variability.

1. INTRODUCTION

It is well known that the solar ultraviolet flux varies in magnitude over the 11-year solar cycle and also on time scales characteristic of the evolution and rotation of solar active regions (see review by Lean [1987] and references therein). Short-term irradiance variations arise primarily from the enhanced ultraviolet emissions in plage regions on the solar disk. The enhanced flux in Ly α , for example, can be as much as 40% higher when an especially active plage region occurs than when the Sun is inactive or "quiet." This variation of solar ultraviolet irradiances over time scales of days to months has been observed over the two most recent solar cycles by the AE-C, AE-E, Nimbus 7, Solar Mesosphere Explorer (SME), and other satellites [Lean, 1987] and perturbs the ozone abundance in the stratosphere and mesosphere, due to a combination of effects resulting from changes in O₂ and O₃ photodissociation rates and changes in atmospheric temperature which affects temperature-

dependent reaction rates [Frederick, 1977; Allen et al., 1984; Eckman, 1986a, b].

The response of stratospheric ozone (and in some cases temperature) to solar UV flux variability associated with rotation of active regions in the solar photosphere has been measured in several observational studies [Gille et al., 1984; Chandra, 1986; Hood, 1987]. However, attempts to detect observationally the mesospheric response of ozone have until recently given ambiguous results. Mesospheric ozone is currently believed to respond to solar UV irradiance variations in the wavelength range 1200 Å < λ < 3000 Å with a phase lag of less than a day [Brasseur et al., 1987]. Over a solar rotation period of ~27 days the solar UV flux variation longward of Ly α is typically <10%. At Ly α the amplitude of the flux variation may be as large as 20%. The photochemical time constant for changes in ozone concentration in the mesosphere is short (~100 s in the upper mesosphere), and thus ozone there is highly variable. Because of this rapid variability and the small magnitude of the fractional variation of solar UV flux, the fractional change in ozone concentration in the mesosphere is difficult to detect; to detect unambiguously the response, one must examine large amounts of data.

Two statistical studies of the correlation of SME airglow observations of mesospheric ozone with solar UV fluxes have reported a statistically significant mesospheric ozone response to solar UV variations with a 27-day period and presumably associated with solar rotation [Aikin and Smith, 1986; Keating et al., 1987]. Using a SME data set of 244 days, Aikin and Smith [1986] established a positive correlation between ozone and solar UV flux with a primary period of 27.1 days for the middle atmosphere. In the altitude region between 65 and 70 km and near 50 km, a secondary period of 13.5 days was apparent. Keating et al. [1987], using a larger

¹E. O. Hulburt Center for Space Research, Naval Research Laboratory, Washington, D. C.

²Department of Earth and Planetary Sciences, The Johns Hopkins University, Baltimore, Maryland.

³Department of Physics and Astronomy, The Johns Hopkins University, Baltimore, Maryland.

⁴ST Systems Corporation, Lanham, Maryland.

⁵Earth and Space Sciences Division, Jet Propulsion Laboratory, and Division of Geological and Planetary Sciences, California Institute of Technology, Pasadena.

⁶Atmospheric Sciences Division, NASA Langley Research Center, Hampton, Virginia.

Copyright 1990 by the American Geophysical Union.

Paper number 90JD02086.
0148-0227/90/90JD-02086\$05.00

SME data set of 622 days, detected an ozone response to solar UV variations throughout the 0.5- to 0.05-mbar (approximately 55- to 85-km altitude) region of the mesosphere. Both studies used the magnitude of the solar Ly α flux as an indicator of solar UV variability.

In the statistical study performed by *Keating et al.* [1987], ozone concentration, solar flux, and atmospheric temperature were analyzed in terms of "ratios" of averages of these observables, that is,

$$R(X) = (X - \bar{X})/\bar{X} \quad (1)$$

where X is a 5-day running mean of a particular observable (e.g., O₃ density or solar Ly α flux) and \bar{X} is a 27-day running mean of X . This function represents a statistical filter that enhances variations that occur near the 27-day period and suppresses shorter- and longer-term variations. The ozone response as defined by *Keating et al.* [1987] is $R(\text{O}_3)/R(F_{\text{Ly}\alpha})$. The statistically inferred mesospheric ozone response, as shown in Figure 13 of *Keating et al.* [1987], clearly shows structure in the 60- to 85-km-altitude region. The response is positive below 63 km and above 78 km and negative in the intermediate altitude region.

Previous theoretical work by *Frederick* [1977] and *Garcia et al.* [1984] predicted a negative ozone response to an increase in UV solar flux, peaking near 70 km. *Garcia et al.* [1984], who investigated the response to the 11-year solar cycle variation, limited the location of negative ozone response to the 70-km region, with a strong positive response at higher altitudes peaking at 80 km. According to *Frederick* [1977] however, the response was negative throughout the mesosphere. The key difference between the two studies is that *Frederick* [1977] had a fixed water vapor profile, while *Garcia et al.* [1984] allowed the water vapor profile in their model to respond to the solar flux changes. Although the *Garcia et al.* [1984] results are in better agreement with the *Keating et al.* [1987] analysis, they substantially overpredict the magnitude of the observed ozone response maximum near 80 km.

Frederick [1977] and *Garcia et al.* [1984] both calculated the response for effective times much longer than the 27-day flux variation, essentially the asymptotic response. Thus an adjustment of the atmosphere, which may occur as a response to the enhanced flux and which has a characteristic process time scale comparable to 27 days, would not be fully evident in these calculations, for example, tracer transport by diffusive processes with a time scale of the order of 2 weeks in the middle mesosphere.

In their study of mesospheric and lower thermospheric ozone, *Allen et al.* [1984] performed a systematic investigation of the sensitivity of O₃ to changes in various atmospheric parameters, including solar illumination conditions and changes in spectral output of the sun [see *Allen et al.*, 1984, Table 3]. Their steady state results incorporated the response of the abundances of transportable constituents, specifically water vapor, to changes in solar irradiance. For variability in solar illumination, both for changes in season and over an 11-year cycle, *Allen et al.* [1984] found a positive correlation between solar flux and ozone above 80 km. At 80 km their calculated change in ozone abundance was 10% and larger at higher altitudes. Below this altitude their calculated response was less than 1%. This result above the 80-km-altitude level is at variance with *Frederick* [1977], but is consistent with *Garcia et al.* [1984], and illustrates the

necessity of incorporating the response of transportable constituents to variability in solar illumination in model studies of the ozone response.

Eckman [1985, 1986a, b] modeled the time-dependent ozone response primarily in the region below 70 km and obtained results in partial agreement with SME measurements of the ozone response. This theoretical study explicitly included time dependence of photochemical processes in the model of ozone response to solar flux variations. However, the distributions of H₂O and H₂ were specified rather than calculated in this model, which limits the applicability of the *Eckman* [1986a] model to middle and upper mesosphere ozone responses since photodissociation of water vapor is the source of odd hydrogen species which catalytically destroy ozone.

Brasseur et al. [1987] also investigated the theoretical response of ozone to solar flux variations with a one-dimensional photochemical radiative time-dependent model of the upper stratosphere and lower mesosphere and found substantial agreement between model results and the data analysis of *Keating et al.* [1987]. The *Brasseur et al.* [1987] model also included a specified constant water vapor mixing ratio with altitude and no variation of water vapor abundance with solar irradiance. Above ~65 km the water vapor abundance falls sharply due to photodissociation from solar UV radiation, primarily Ly α , and a realistic model of the ozone response in this region of the atmosphere must include realistic water vapor abundances.

In the lower mesosphere (below 60 km) and upper stratosphere the observations of the ozone and solar UV correlation are in substantial agreement with simple photochemical models [*Hood*, 1987; *Hood and Douglass*, 1988]. Both the amplitude and phase of the response in this region of the atmosphere can be accurately described when the observed temperature response is incorporated into such models [*Hood and Douglass*, 1988].

In light of the recent detection of a 27-day mesospheric ozone periodicity [*Keating et al.*, 1985, 1987], we performed a detailed one-dimensional modeling study of the mesospheric ozone response to solar UV flux variations to remove some of the deficiencies in previous studies and to examine specifically the importance of solar zenith angle, self-consistent calculation of water vapor abundance, and temperature feedback with a non-local thermodynamic equilibrium (non-LTE) radiation model. The goal of this paper is to determine the relative importance of several modeled processes in controlling the magnitude and phase of the mesospheric ozone response.

The plan of this paper is as follows. In section 2 we describe the photochemical model used to study mesospheric chemistry and the response of chemistry and constituent profiles to solar flux variations. We discuss the assumptions made for the purpose of comparing model results with the *Keating et al.* [1987] ozone response. Section 3 contains numerical results for the theoretical ozone response. At the end on section 3 we show the results of selected time-dependent calculations to illustrate the degree to which a relatively simple model of the mesosphere such as used here is able to capture the major characteristics of the observed response. A summary of the major conclusions and implications of this study is made in section 4.

2. THEORETICAL MODEL

The one-dimensional photochemical model developed at California Institute of Technology and described in detail by Allen *et al.* [1981, 1984] was used in this study. It incorporates vertical transport by eddy and molecular diffusion and updated (Jet Propulsion Laboratory (JPL-1987)) kinetic rate constants [Strobel *et al.*, 1987]. The lower boundary of the model was selected to be at 40-km altitude, and because ClO_x and NO_x chemistry is not included, the model solutions are deemed reliable above ~55 km. The upper boundary was chosen to be 130 km. The calculations adopted diurnal averaging of atmospheric transmission functions in the UV and visible regions of the solar spectrum. In this paper, photochemical reactions will be referred to with the same numbering scheme given by Allen *et al.* [1981]. The baseline reference model (case A) is in all essential respects model C of Strobel *et al.* [1987]. The time-dependent temperature calculation part of the model is described in section 3.2.

The background atmosphere was adopted from Barnett and Corney [1985] for altitudes between 0 and 80 km, extended to 120 km using both the Air Force Geophysical Laboratory (AFGL) model of Cole and Kantor [1978] and the data of Forbes [1985]. As mentioned in section 1, the statistical study of Keating *et al.* [1987] includes almost 2 years of data at many latitudes and as such introduces a problem in the choice of an appropriate background atmosphere for our one-dimensional model calculations. An examination of the atmospheric data base showed that near equinox, the vertical profiles of temperature and total density have a relatively small variation over a wide range of latitudes. Also, atmospheric pressure and temperature fields near equinox are generally midrange between the values at solstices for mid-latitude regions. Thus we chose a monthly average temperature and total density profile appropriate for March and 33°N for the background atmosphere in this paper, although in some future study, background atmospheric variations may have to be considered. This particular choice of latitude will be discussed below.

The ozone response curve shown in Figure 13 of Keating *et al.* [1987] incorporates a large amount of data, covering almost 2 years in time and ±40° in latitude. Since it would clearly be prohibitive to make enough model runs to reproduce even partially this data set, some simplifying assumptions are necessary. In particular, only the effects of variations in the magnitude of the solar flux and solar zenith angle (χ) are considered. The one-dimensional model, when used to represent diurnally averaged conditions, has been shown [Allen *et al.*, 1984] to give results which are appropriate for a local time of approximately 1500, the time of SME observations [Thomas *et al.*, 1984]. We ran the model under solar illumination conditions that give effective average solar zenith angles (χ) at 1500 LT of 45°, 55°, 65°, and 75°. In Table 1 we show the probability of the occurrence, in the Keating *et al.* [1987] data set, of a solar zenith angle (χ) at 1500 LT, within the tabulated 10° bins. More than 98% of the expected solar zenith angles are less than 80°. For purposes of comparison between the Keating *et al.* [1987] observed ozone response and the photochemical model, we used a weighted sum of model runs made at the above selected zenith angles, where the weights are obtained from Table 1. We have found that in general, the weighted sum of the

TABLE 1. Zenith Angle Probability of Occurrence

Range of χ	Probability of Occurrence
40–50	0.517
50–60	0.233
60–70	0.144
70–80	0.089
80–90	0.017

model results differs little from a single diurnally averaged run with a zenith angle at 1500 LT of 55°. At equinox this occurs at latitude 33°N.

The SME instruments measured ozone and solar flux on a daily basis. The solar irradiance spectrometer range covers our region of interest (1200–3000 Å) in the solar spectrum. SME solar flux measurements for the time period January 1982 through December 1983 were averaged to form the baseline solar flux profile, $F_{\text{ref}}(\lambda)$. This is the same time period covered by the SME ozone data analyzed by Keating *et al.* [1987]. We ignored the solar flux variation for wavelengths outside of the above wavelength range, since deposition of solar radiation for wavelengths below 1200 Å is only significant in the thermosphere, and solar flux variations over a solar rotation period above 3000 Å are too small (less than 1% [see Lean, 1987]) to be important.

An attempt was made to correlate the SME solar flux at Ly α with all other wavelengths within the above wavelength range, using the Keating *et al.* [1987] parameter R as a variable. This provided a variation curve with complex structure. The correlation coefficients of the regression fits become poor for wavelengths longer than about 2000 Å. However, the essential physics associated with this correlation can be represented by a function for the amplitude of the solar flux variation over a solar rotation with monotonic dependence on wavelength.

From a statistical study of the solar flux variation with rotation over many solar rotations and using a number of data sets including SME, Lean [1987] deduced the average solar rotational modulation of ultraviolet irradiance within selected wavelength intervals. The solar rotational modulation is simply the maximum percentage variation in irradiance during a solar rotation. The observed rotational modulation of the solar irradiance at selected wavelengths is <1% at 3000 Å, 2.5% at 2500 Å, 6% at 2000 Å, 16% at 1500 Å, and 40% at 1216 Å. Using these values (reduced by a factor of 2 to give an amplitude for the assumed periodic solar flux variation), we generated a smoothly varying function with wavelength to represent the amplitude of the periodic solar UV flux variation. Over the time period of the SME observations used by Keating *et al.* [1987], the amplitude of variation was about half that deduced by Lean [1987]. We therefore reduced the above fractional variation by another factor of 2 for use in the model calculations. This gave an amplitude for solar flux variation over a “typical” solar rotation period at Ly α of approximately 10%. The factor by which the solar flux is multiplied to obtain the maximum during a solar rotation period is shown as the dashed curve in Figure 1. At Ly α the average solar flux over this time period was 3.23×10^{11} photons cm⁻² s⁻¹.

Two solar flux profiles were used for the asymptotic model calculations of the ozone response: the baseline profile $F_{\text{ref}}(\lambda)$ and the baseline profile multiplied by the assumed

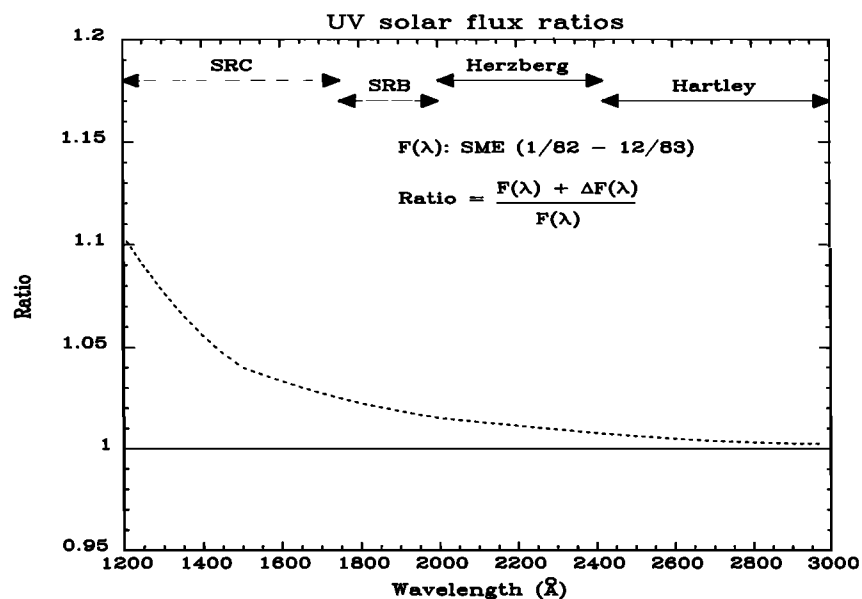


Fig. 1. Ratio of perturbed solar flux profile (dashed curve) to baseline SME solar flux profile (averaged from January 1982 to December 1983) between 1200 and 3000 Å adopted for the calculations.

relative variation factor given in Figure 1 to give $F_{\max}(\lambda)$. The fractional variation of solar Ly α flux is defined by

$$\frac{\Delta F_{\text{Ly } \alpha}}{F_{\text{Ly } \alpha}} = \frac{F_{\max}(\text{Ly } \alpha) - F_{\text{ref}}(\text{Ly } \alpha)}{F_{\text{ref}}(\text{Ly } \alpha)} \quad (2)$$

We define the ozone response to be

$$\frac{\Delta O_3}{O_3} = \frac{[O_3]_{\max} - [O_3]_{\text{ref}}}{[O_3]_{\text{ref}}} \quad (3)$$

where $[O_3]$ represents the ozone density. As will be shown later, if one scales the ozone response by the assumed fractional solar flux variation at Ly α , the result is relatively insensitive to both the absolute magnitude of the solar fluxes and to the amplitude of the Ly α variation adopted in the calculations. In what follows we will calculate the ozone response in this manner, and for comparison with the observations of Keating *et al.* [1987], we present this response normalized by the fractional variation of solar flux at Ly α .

3. MODEL RESULTS

3.1. Sensitivity Study

We begin by looking at the steady state ozone response for two reasons. First, this investigation is aimed at determining which of several processes are most responsible for characterizing the response of ozone to solar flux variations in the mesosphere and are not primarily interested in obtaining a detailed "fit" to observations. Rather, we are exploring the sensitivity of the ozone response to selected parameters, and steady state calculations are adequate for this purpose. Second, the steady state response is computationally about 2 orders of magnitude faster than calculations of the time-dependent response. After exploring the relative magnitude of differing assumptions on the magnitude of the steady state response, we will show results (section 3.1.6) for a time-dependent calculation of the response to a step function

increase in solar flux. In section 3.2 we will present time-dependent calculations of the coupled ozone and temperature response to time-varying solar flux variations.

In order to calculate the steady state response we first calculate the steady state distribution of species with the baseline solar flux profile and then the steady state distributions with the increased solar flux profile. We define the asymptotic ozone response to be the fractional change in ozone concentration between the two cases (equation (3)). In Table 2 we list the model cases considered and the key assumptions for each. The reference model, case A, incorporates standard JPL stratosphere/mesosphere chemistry (JPL-1987) and an eddy diffusion coefficient (K_{zz}) which was found to provide satisfactory agreement between the model H₂O vertical mixing ratio profile and recent microwave measurements of mesospheric water vapor, i.e., model C of Strobel *et al.* [1987].

3.1.1. *Wavelength-dependent UV flux variations.* The sensitivity of the calculated ozone response to solar flux variations in individual wavelength intervals is shown in Figure 2 for model A, where we have chosen solar illumination conditions which correspond to 1500 LT solar zenith angle of 55°, and the solar UV flux is increased over the

TABLE 2. Summary of Model Cases

Model Case	Description
A	reference case (JPL-1985 chemistry)
B	HO _x rate coefficient modifications [Rusch and Eckman, 1985]
C	Bevilacqua <i>et al.</i> [1987] water vapor profile
D	temperature-chemistry (T-C) feedback effect
E	time-dependent response, step function in ΔF , no T-C feedback
F	time-dependent response, step function in ΔF , T-C feedback
G	time-dependent response, sinusoidal $F_{\lambda}(t)$ forcing, T-C feedback
H	time-dependent, sinusoidal $F_{\lambda}(t)$, specified $T(t)$

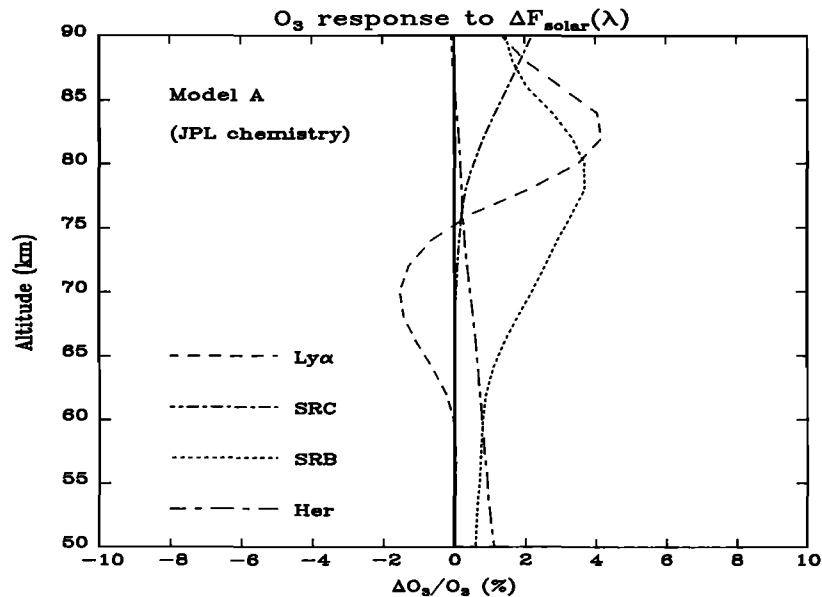


Fig. 2. Ozone response for changes in solar UV flux within discrete wavelength intervals of the solar spectrum. The change in solar flux within the intervals is equal to the ratio shown in Figure 1. The wavelength intervals are defined in the text. Calculations were made at a zenith angle of 45°.

baseline flux by a factor equal to the ratio plotted in Figure 1 within specific wavelength regions. The four wavelength regions are shown at the top of Figure 1 and are labeled SRC (1200–1750 Å), SRB (1750–2000 Å), Herzberg (2000–2425 Å), and Hartley (2425–3000 Å). In Figure 2 we show the effect of varying the flux within the first three ranges and a case where we have varied the flux only within the Ly α line. For a much more detailed discussion of mesospheric chemistry and of the atmospheric regions that are most sensitive to the solar UV flux in these regions of the solar spectrum, the reader is referred to the works by Allen *et al.* [1981, 1984], Clancy *et al.* [1987].

It is clear from Figure 2 that the greatest response above about 63 km is due to the Ly α flux variation (except for a very narrow region at 75 km). In the region between 65 and 75 km the increased Ly α solar flux enhances the photodissociation of water vapor and hence increases the density of odd hydrogen (HO_x). This effect peaks near 70 km where unit optical depth for Ly α penetration through overlying absorbing molecular oxygen occurs. Above 75 km there is insufficient HO_x production to overcome increased Ly α photodissociation of molecular oxygen (odd hydrogen still plays a role in determining the ozone density to about 82 km). Thus, at 85 km where increased net production of odd oxygen maximizes, there is a peak in the ozone response.

Above 75 km the ozone response to increased solar flux is complex, with Ly α , Schumann-Runge continuum, and Schumann-Runge band regions all contributing in significant amounts, through enhanced odd oxygen production. Below 65 km, penetration of solar photons in the Schumann-Runge bands and Herzberg continuum produces a net positive ozone response, since insignificant water vapor photodissociation occurs that low in the atmosphere. The effect of varying the solar flux in the Hartley region of the solar spectrum by the assumed ratio function produces a negligible ozone response. It should be noted that the magnitudes of the ozone response profile's maxima and minima are

similar to those shown by Garcia *et al.* [1984] in both location and degree.

Figures 3b and 3c show the fractional change in photodissociation rate coefficients and rates, for the photodissociation pathways for O₂, O₃, and H₂O, respectively. Note that although the fractional changes may be large (~10%), e.g., Ly α dissociation of



the reaction may be of minor importance in the photochemistry over an extended altitude range (e.g., H₂O below 65 km). Note that the net fractional change in the water vapor photodissociation rate coefficient is positive and large throughout the upper mesosphere and also that the water vapor abundance profile has decreased slightly (see Figure 3a) as a result of the increased solar flux. As a result, the net rate of water vapor photodissociation has decreased above about 81-km altitude. This illustrates the necessity of incorporating the response of the water vapor abundance profile to solar flux changes in order to model accurately the response of ozone to solar flux changes.

3.1.2. *Solar flux and zenith angle variations.* The calculated ozone response for several solar illumination conditions (effective solar zenith angles) is shown in Figure 4. Here we have normalized the calculated ozone response by the fractional change in Ly α flux for the purposes of comparison with the data analysis of ozone response by Keating *et al.* [1987] which is plotted on our altitude grid [see Keating *et al.*, 1987, Figure 13]. The Keating *et al.* [1987] response is shown for reference only in the following figures, and conclusions regarding a comparison between model results and this observed response will be discussed later. The calculated ozone response is a strong function of effective solar zenith angle. The negative response maximum increases in altitude from 67 km at a zenith angle of 45° to 72 km at 75°. The variations in the altitude of the ozone negative response maximum with increasing latitude are also in

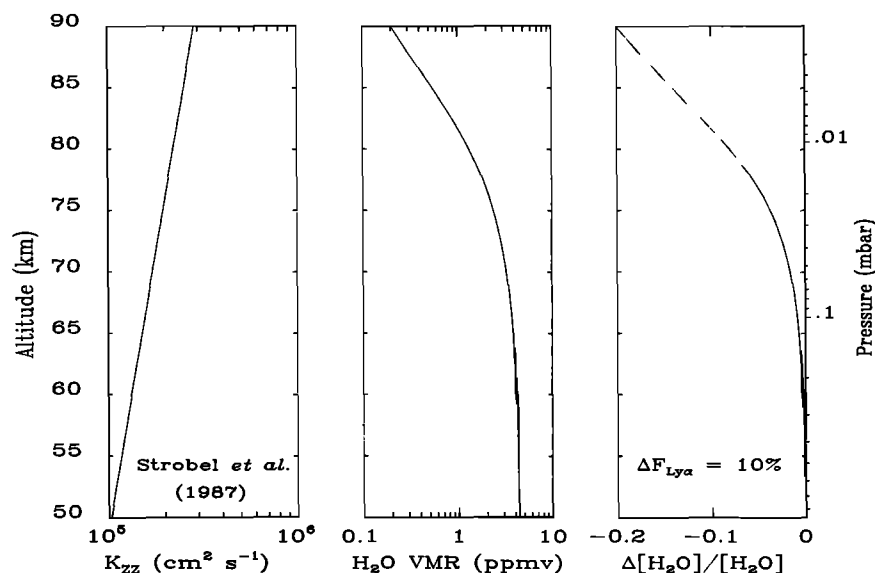


Fig. 3a. (Left) The baseline vertical profile of eddy diffusion coefficient (K_{zz}) used model calculations. (Middle) The corresponding calculated water vapor mixing ratio. (Right) The fractional change in water vapor abundance (ppmv) for model A.

agreement with the Garcia *et al.* [1984] results. This is a general result for most of our calculated asymptotic responses using spring water vapor concentration profiles [Bevilacqua *et al.*, 1983, 1987]. The small positive response below 60 km, roughly constant with altitude is relatively insensitive to the solar zenith angle, i.e., invariant with latitude. The calculated ozone response is dependent upon the assumed baseline Ly α flux level, which varied from ~ 2.5 to $4.5 \times 10^{11} \text{ cm}^{-2} \text{ s}^{-1}$, over the time period in which SME measurements were made. We performed calculations with Ly α baselines over this range and found the response (not shown) below 60 km nearly the same in all cases, within model determinations. Between 60 and 70 km, a factor of 1.6

increase in the flux level lowers the altitude of the maximum negative response about 2 km and increases its magnitude by about 15%. Above 70 km the response is more sensitive; at the peak in the positive response the variation is about 30%. The important point is that the character of the response curve is basically insensitive to the magnitude of the solar UV photon flux.

As noted in section 1, the amplitude of variation of solar irradiance depends on the "activity" of the plage regions in the solar atmosphere. Thus the amplitude of irradiance variation will vary from one solar rotation to the next. On the basis of the study of Lean [1987] the rotational solar flux amplitude variation at Ly α ranges between 5 and 30%. Over

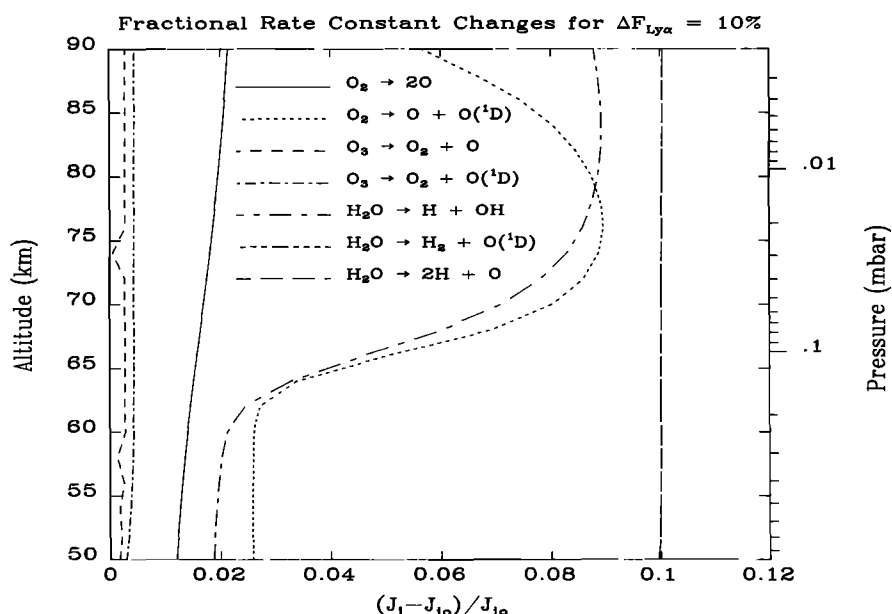


Fig. 3b. Fraction change in photodissociation rate constants for a fractional change in the incident solar flux profile shown in Figure 1. The last two reactions have identical changes.

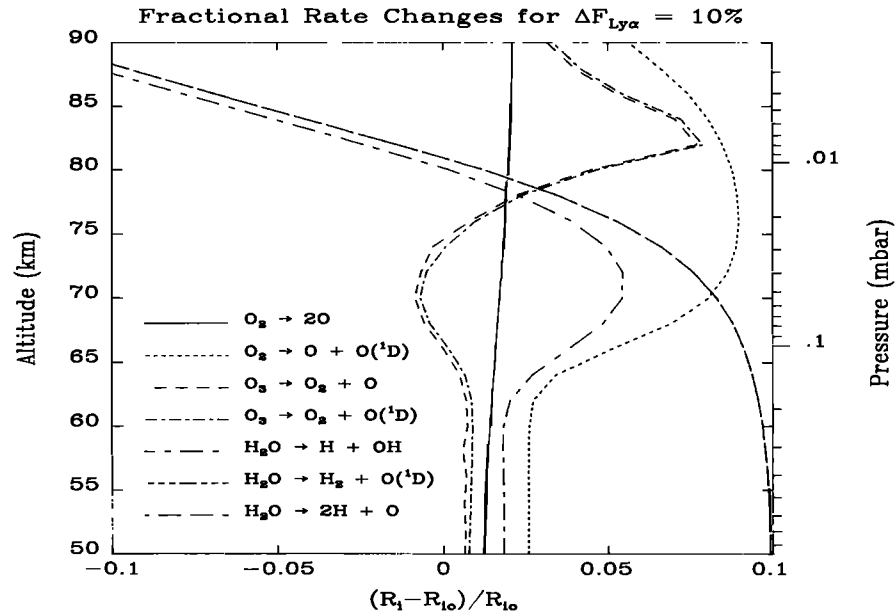


Fig. 3c. Fractional change in photodissociation rates for the fractional increase in solar flux shown in Figure 1. The last two reactions have identical changes.

this range of amplitude variation we find that (simulations not shown) the ozone change is nearly linear; thus there is negligible change in the calculated ozone response when normalized by the flux in Ly α . This supports the validity of our method for performing these calculations and comparing with mesospheric data. Normalizing to the solar flux at the Ly α line removes the almost certain variation of solar flux amplitude with wavelength from one solar rotation to another.

3.1.3. *Ozone chemistry.* The ozone density in the mesosphere is a strong function of the kinetic reaction rates for the HO_x catalytic cycles which remove ozone [Allen et al.,

1981, 1984], and various proposals involving modifications of these rates and other key rates involving net odd oxygen production have been put forward as attempts to explain the model/data discrepancies of ozone in the mesosphere and lower thermosphere [Rusch and Eckman, 1985; Strobel et al., 1987; Clancy et al., 1987]. We have incorporated the Rusch and Eckman [1985] changes in the calculation of ozone response in model B. As seen in Figure 5, these changes yield only a slight decrease in the magnitude of the calculated ozone response, with a maximum decrease in the positive ozone response at 83 km of less than 20%. Similar model runs were made with the additional changes recom-

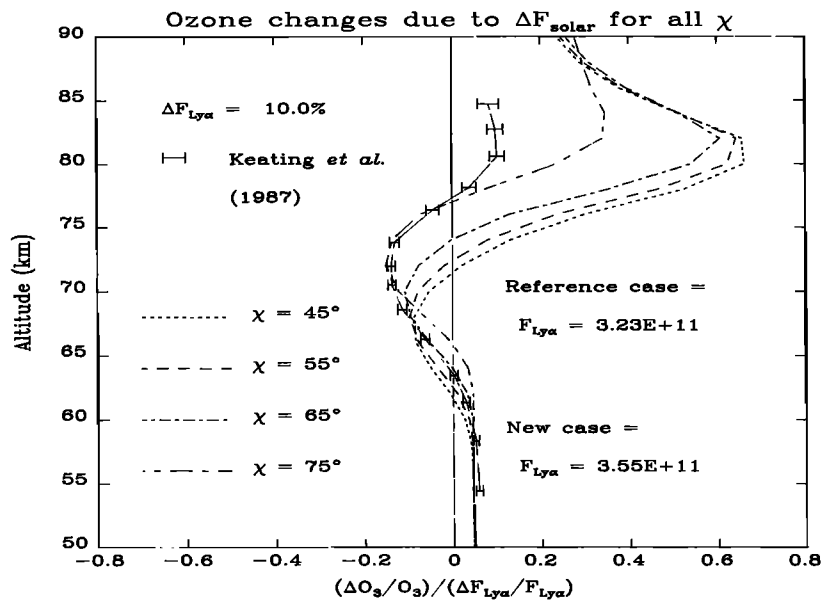


Fig. 4. Ozone response calculated for four separate zenith angles with a 10% change in solar flux at Ly α . The ozone response normalized to the Ly α fractional variation as determined by a statistical analysis of SME data [Keating et al., 1987] is shown for comparison.

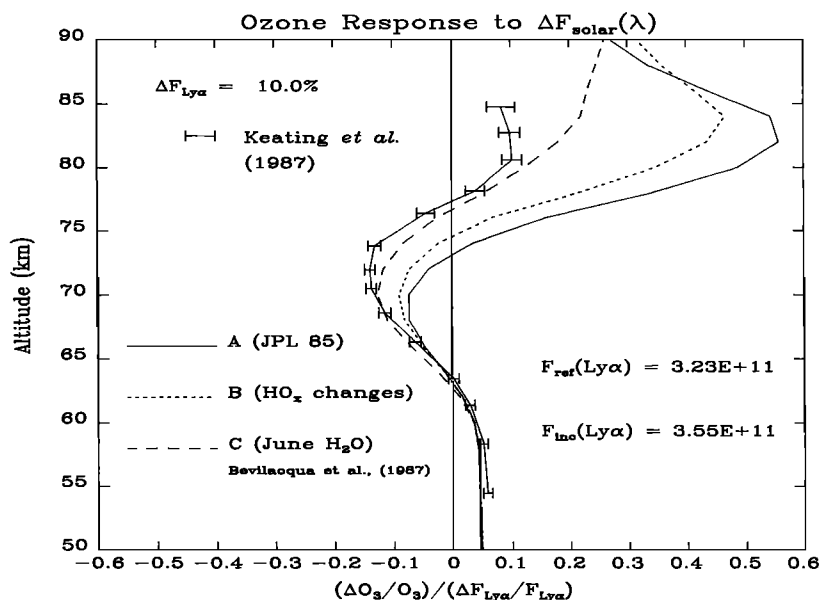


Fig. 5. Ozone response for the reference model (model A, solid curve), for the case where the efficiency of the HO_x catalytic loss of ozone has been decreased according to the recommendations of *Rusch and Eckman* [1985] (model B, short dashed curve), and for the case where the water vapor is increased high in the mesosphere to match the June data of *Bevilacqua et al.* [1987] (model C, long dashed curve).

mended by *Clancy et al.* [1987] (in their models A and B). These model runs produced results almost identical to those shown for our model B. Thus one can conclude that these suggested modifications in mesospheric ozone photochemistry may be sufficient to alleviate model/data discrepancies in ozone abundances but do not affect in a significant way the prediction of the ozone response to solar flux changes expected during a solar rotation.

3.1.4. *Water vapor abundance.* The mixing ratio of water vapor at 80 km is 1.6 parts per million by volume (ppmv) for model A and is consistent with ground-based microwave measurements of water vapor which represent an average for the time period April–June 1984 at JPL [*Bevilacqua et al.*, 1985]. More recent microwave measurements of mid-latitude mesospheric water vapor at Penn State, which encompass the months November–July, show substantial seasonal variation of upper mesosphere water vapor [*Bevilacqua et al.*, 1990], with December, April, and June values of 1.0, 1.6, and 2.9 ppmv, respectively, at 80 km.

In model C we have increased the magnitude of the background vertical mixing to give 3 ppmv of water vapor at 80 km, with a vertical gradient in water vapor mixing ratio from 60 to 80 km that is similar to that for the June water vapor measurements [*Bevilacqua et al.*, 1990] and the water vapor profile used in the model calculations of *Allen et al.* [1981]. The abundance of water vapor in model C is large enough that enhanced Ly α flux produces an increase in reactive HO_x sufficient to generate a net increase in the catalytic loss of ozone up to 80 km, thus reducing the ozone response shown in Figure 5. A model run was performed to simulate the winter conditions with ~ 1 ppmv at 80 km. Although the water vapor abundance was smaller than the value for the model A, the calculated response was almost identical, which indicates that there is an effective threshold value of the water vapor abundance above which there is the onset of negative ozone response in the region above 80 km.

This threshold is approximately 1.5 ppmv at 80 km, typical of spring microwave measurements [*Bevilacqua et al.*, 1990]. We therefore infer that the ozone response to solar UV flux variations should be seasonally variable through the seasonal variation of water vapor abundances.

3.1.5. *Temperature-chemistry feedback.* Temperature in the stratosphere and mesosphere is intimately connected to the ozone distribution. Variabilities in ozone concentration and local atmospheric temperature are likewise related to a phase lag which depends on altitude [*Brasseur et al.*, 1987; *Keating et al.*, 1987; *Mohanakumar*, 1985; *Hood*, 1987; *Hood and Douglass*, 1988]. Although the phase lag may be as long as weeks in the middle stratosphere, the phase lag in the upper mesosphere is much shorter than the solar rotational period [*Brasseur et al.*, 1987].

The inverse temperature dependence of ozone has been observed in the mesosphere and upper stratosphere by *Aikin and Smith* [1986] and has been investigated with a one-dimensional radiative and photochemical model (not including transport) by *Eckman* [1985]. For the region above about 75 km where ozone chemistry is relatively simple this negative feedback may be described as follows. A positive ozone response will lead to a local increase in the heating rate, since ozone and molecular oxygen are the primary absorbers of solar UV energy in this region of the atmosphere [*Strobel*, 1978]. Here the atmosphere is in approximate radiative equilibrium on a globally averaged basis; thus an increase in heating leads to an increased temperature, with a time lag of the order of 1 day at 80 km [*Brasseur et al.*, 1987].

To first order, an increase in temperature has two kinetic effects. Increased temperature results in a lower kinetic rate coefficient for three-body recombination of atomic and molecular oxygen, that is,

Reaction (R54) of *Allen et al.* [1981]

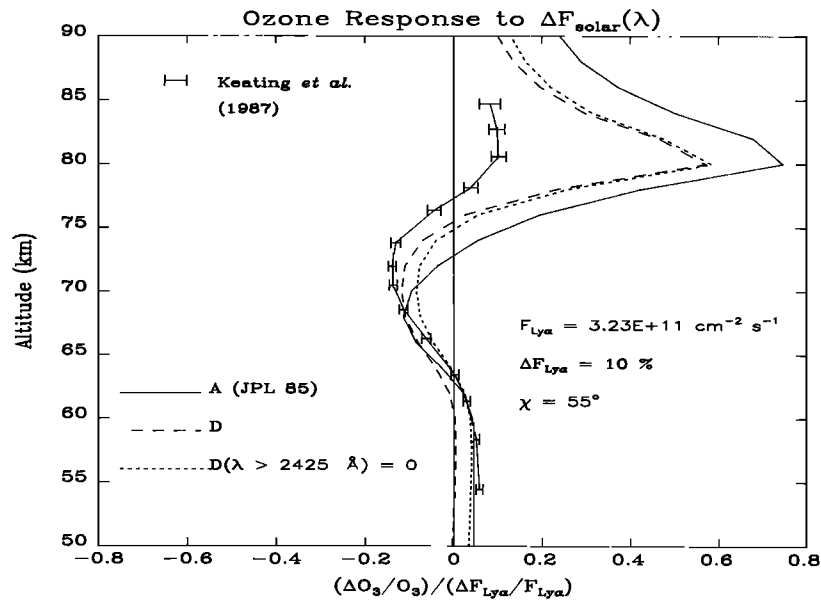
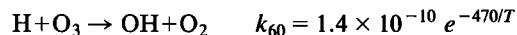


Fig. 6. Ozone response without temperature feedback (solid curve), with temperature feedback (short dashed curve), with temperature feedback but Hartley region variation suppressed (long dashed curve), all assuming local radiative equilibrium and temperature response calculated as described in the text.



and a higher rate coefficient for the two-body reaction of atomic hydrogen and ozone

Reaction (R60) of Allen *et al.* [1981]



[see Allen *et al.*, 1981, 1984]. Both of these effects serve to moderate the effect of an increased production of atomic oxygen by photodissociation of O₂, thus suppressing ozone density variations due to solar UV flux variations.

Temperature feedback is difficult to model accurately in the mesosphere because of the complexity of the non-LTE nature of the IR radiative transfer. We constructed a time-dependent model for temperature profile where heating is due to absorption of solar energy by O₂ and O₃ and cooling is by 15- μm bands of CO₂. We calculate the time-dependent atmospheric temperature from the equation

$$\rho c_p \frac{dT}{dt} = H(t) - C(t) \quad (4)$$

where ρ is the mass density of the atmosphere and c_p is the atmospheric heat capacity. The time-dependent heat equation is solved for atmospheric temperature in a manner similar to that of the time-dependent chemical continuity equations; that is, we time step equation (4) forward in time. We used the parameterization of Strobel [1978] to calculate the heating rates. The non-LTE cooling by CO₂ is calculated by the Curtis matrix formalism described by Zhu and Strobel [1990a, b]. The baseline model atmosphere in our calculations is assumed to be in radiative equilibrium at the observed temperature. Perturbations on the temperature field lead to perturbations in the net cooling represented by a matrix (generated from the baseline atmosphere) operating on the vector defined by the temperature perturbation [see

Zhu and Strobel, [1990b, equation (8)]. At each time step, new oxygen and ozone densities are calculated in response to the updated temperature field, which are then used to update the new heating and cooling rates to time step the temperature equation.

We show the asymptotic response with temperature feedback both with and without an increase in the photon flux in the Hartley region of the spectrum as case D in Figure 6, in comparison to model case A. Above 75 km the normalized ozone response with an increase in the Hartley region is decreased by about 25% over case A when temperature feedback is included. Between 65 and 75 km the temperature feedback has a relatively more dramatic effect on the calculated response. Below 65 km, temperature feedback suppresses the calculated ozone response. This is a result of the assumed 1% increase in solar flux out to 3000 Å. Suppressing this variation in the Hartley region of the spectrum (≥ 2425 Å) has little effect on the ozone response above 73 km, but below 60 km where most atmospheric heating is due to the absorption of solar photons in the Hartley continuum by ozone the positive ozone response is restored with temperature feedback included, albeit at reduced amplitude for ΔT .

Above 80 km the effect is to improve slightly the model/data agreement over case A when temperature feedback was not included. Temperature feedback decreases the positive response near 84 km but not sufficiently to match the data. Between 65 and 75 km the temperature feedback drives the calculated response in the direction to improve the agreement with the Keating *et al.* [1987] data. Below 60 km where most atmospheric heating is due to the absorption of solar photons in the Hartley continuum by ozone, the positive ozone response is obtained with temperature feedback included and suppression of solar flux variation in the Hartley region.

3.1.6. *Time-dependent step function increase in solar UV.* The time evolution of active plage regions in the solar atmosphere is clearly not simple to model. Even for plage

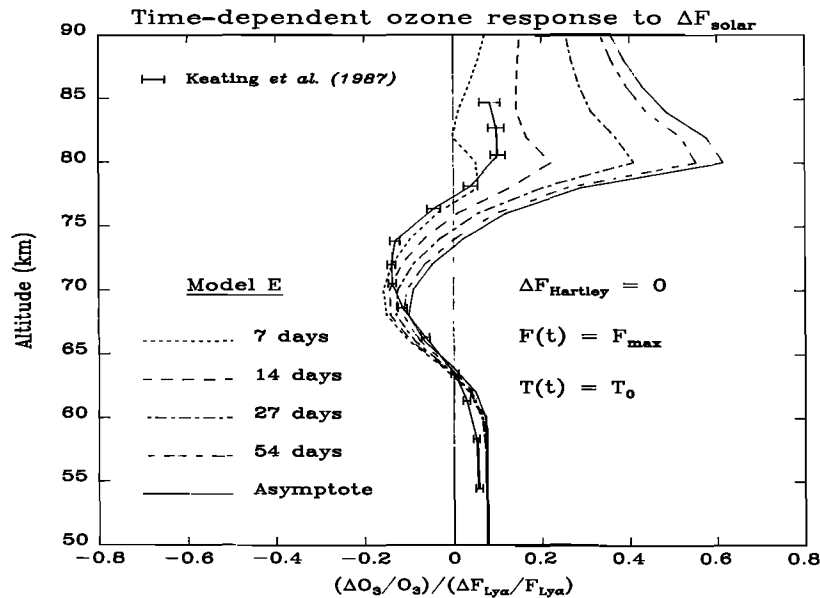


Fig. 7a. Time-dependent ozone response without temperature feedback for a step function increase in solar flux after 7, 14, 27, and 54 days, and the asymptotic limiting response.

regions undergoing little changes in the level of activity over a solar rotation, the exact periodicity will depend upon their solar latitude, since the Sun does not rotate as a solid body. From a study of the periodicity of UV solar flux with solar rotation, *Lean* [1987] found maximum power at time periods of 27 days and 13 days. A single long-lived active region on the solar disk will produce enhanced UV irradiance for several weeks. Thus, ignoring the evolutionary aspects of plages, enhanced UV irradiance may be approximated as either a step function with a step length of half a rotation period or possibly as a sinusoidally varying function with a wavelength of the order of a rotation period. This assumes that only one localized region of the Sun is producing the enhanced UV emission. If several plage regions are active and widely dispersed in solar longitude, then an effective time scale could be much longer than half a rotation period.

We have simulated the time-dependent response of me-

sospheric ozone to solar ultraviolet forcing by time marching the photochemical solution in accord with a step function increase in solar flux. On the basis of the results from model D, we have set the Hartley flux variation to zero in all of our time-dependent calculations. For models E and F (see discussion below) we have simulated the ozone response without (E) and with (F) temperature-chemistry feedback, respectively. We started the time integration at day 1 with a steady state solution calculated with a baseline solar flux level and then at each subsequent time step used the maximum solar flux level and allowed the constituent profiles to respond to the increased solar flux. In Figures 7a and 7b we show results for models E and F, respectively, after 7, 14, 27, and 54 days of time integration. The asymptotic response is simply the ratio of the ozone profiles for the steady state enhanced flux solution to the steady state baseline flux solution, also shown in Figure 7.

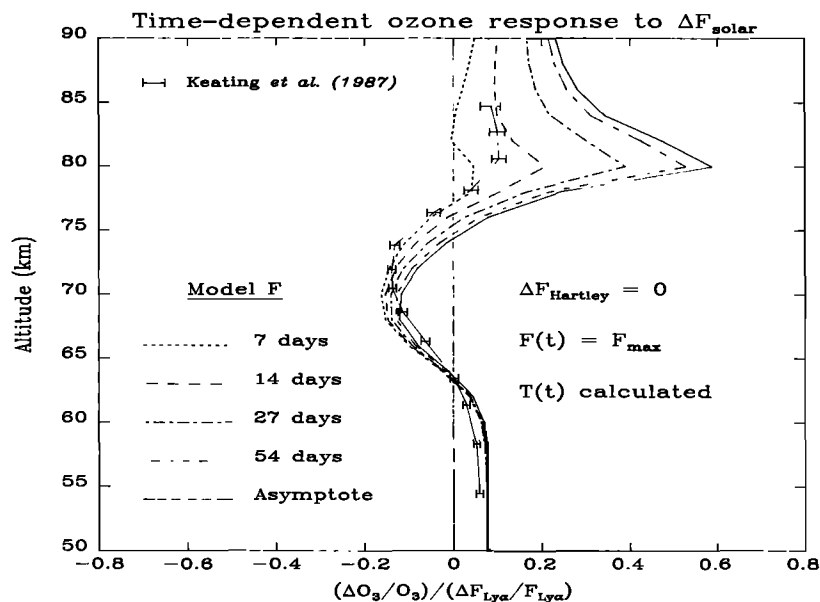


Fig. 7b. The same as Figure 7a but including temperature feedback.

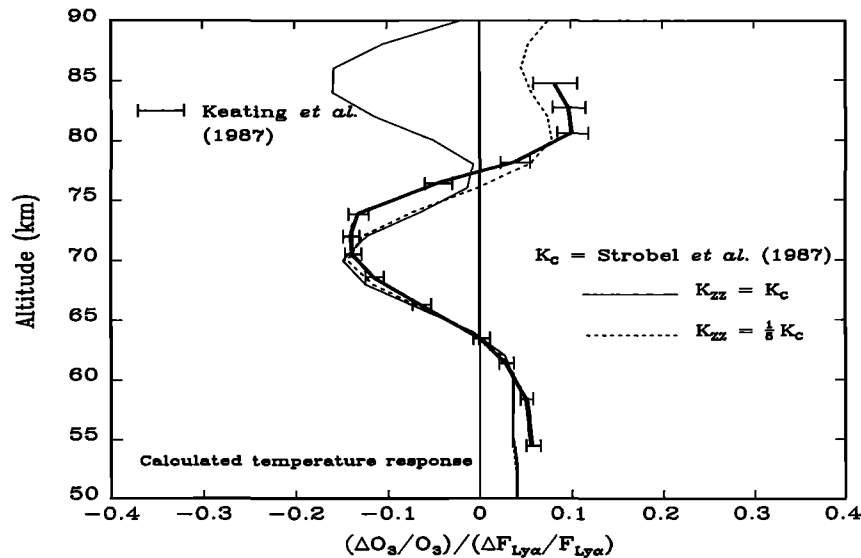


Fig. 8a. Ozone response for a sinusoidal variation of solar UV flux for model G, using the baseline model K_{zz} profile, and K_{zz} decreased by a factor of 5. Temperature response is calculated, and temperature-chemistry feedback is included.

As can be seen from Figure 7a at $t = 54$ days, the ozone distribution has very nearly reached its asymptotic value at all altitudes. Below 65-km altitude the asymptotic response is reached in much less than 7 days. However, for a time period of 7–14 days, characteristic of the time a single active solar plage region is on the visible disk, the ozone response above the 65-km-altitude level is far from its asymptotic limit. For $t = 14$ days the response is only 0.3 of its asymptotic value due to the time-dependent response of the water vapor profile, since the chemical lifetime of water vapor varies from ~ 100 days at the stratopause to ~ 10 days at the mesopause. An increase in the UV flux which dissociates water vapor will depress the water vapor mixing ratio profile. Depressing the water vapor profile above the 75-km-altitude region leads to lower HO_x and hence lower catalytic destruction of ozone. The time scale over which the local water vapor abundance adjusts to an increase in solar UV flux is the transport time scale, of the order of 10 days at 80 km. The time scale for the entire water vapor vertical profile is somewhat longer since it is an integrated effect down to about 65 km. It is clear that the results for model integrations for 7 and 14 days encompass the mesospheric response as deduced by Keating *et al.* [1987].

The effect of temperature-chemistry feedback on the time-dependent ozone response is similar to that for the asymptotic cases. The temperature increase due to increased ozone densities near 80 km moderates the ozone response by about 30%, as is seen in Figure 7b.

The results presented above illustrate the sensitivity of the calculated ozone response to various model parameters. Of all the above changes, the water vapor abundance, temperature-chemistry feedback, and time dependence appear to dominate the ozone response. The seasonal variability of mesospheric water vapor is large at mid-latitudes [Bevilacqua *et al.*, 1989]. Also, the exact time dependence of solar flux on a 27-day time scale is variable from one solar rotation to the next. Both of these variables should be accurately known to describe in detail the response of mesospheric ozone to solar irradiance variations.

3.2. Periodic Solar UV Flux Variation

The time scale for changes in plage activity is of the order of half a solar rotation. During this time, plages can form and disintegrate. For solar activity of this sort a more proper description of solar UV flux variation might be of a sinusoidal nature. A periodic variation of incident solar flux on the mesosphere will produce a predominantly instantaneous response from ozone and a delayed atmospheric water vapor and temperature response at all altitudes. In order to model the effect of a sinusoidal UV forcing, we considered two cases with temperature-chemistry feedback. In the first we calculated the temperature response as described above. The second is a calculation of the ozone response with a specified temperature response: the observed temperature amplitude and phase of Keating *et al.* [1987]. The principal uncertainty is the water vapor abundance. We calculated the mesospheric water vapor abundance as implied by specified vertical profiles of the eddy mixing rate parameterized by the coefficient K_{zz} . Below we investigate the influence of the magnitude of eddy mixing on the calculated ozone response.

3.2.1. Calculated temperature response. For model case G a sinusoidal 27-day variation of solar ultraviolet flux was chosen, and the time-dependent temperature was obtained from equation (4). The eddy diffusion coefficient profile is identical to model C of Strobel *et al.* [1987]. The results for this case are shown as the solid curves in Figures 8a–8d. Below 75-km-altitude the calculated response (Figure 8a) is quite similar to the 14-day response in model case F, as expected, since a sinusoidal forcing can be crudely approximated by half period step functions. The water vapor abundance is out of phase with the solar flux forcing. Below 75 km the fractional change in water vapor is much smaller than the fractional change in solar flux (Figure 3a), so an increase in solar flux to first order only changes the abundance of HO_x species that are in photochemical equilibrium with H_2O . But the water vapor below 75 km does not vary significantly over a 27-day period; thus the ozone response is not changed significantly over longer integration times.

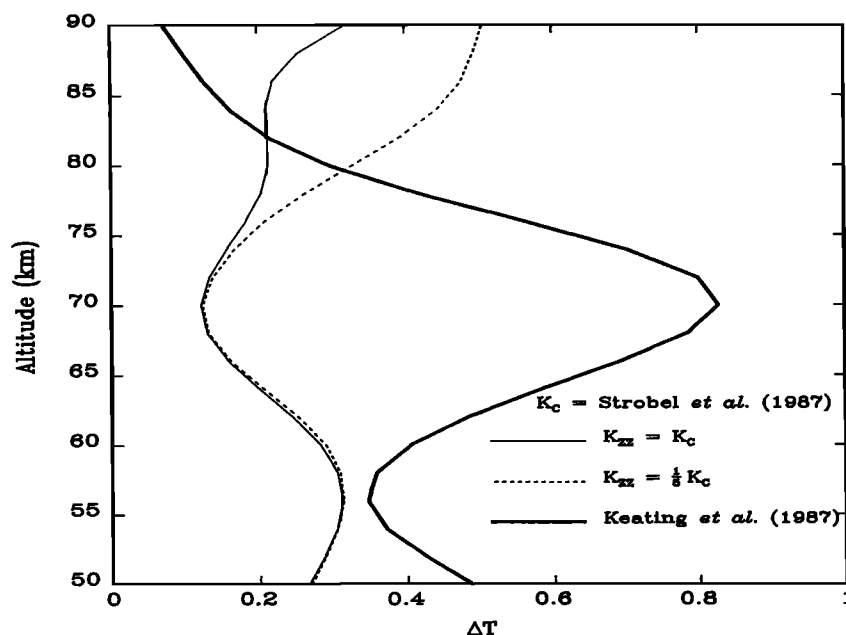


Fig. 8b. Temperature response amplitude for corresponding K_{zz} profiles. Plotted in the dark solid curve is the Keating *et al.* [1987] 2050-Å observed amplitude response.

Above 75 km, however, the fractional change in water vapor abundance becomes quite large, as seen in Figure 3a. Moreover, the magnitude of the change depends upon the length of time the solar UV flux is greater than the baseline value. For periodic solar forcing of a period of 27 days the water vapor perturbation above 80 km reaches less than half that for the asymptotic limit. The strong negative ozone response to an increase in solar UV flux above 78 km requires a significant water vapor abundance and a sluggish response to solar forcing such that it is far away from its asymptotic value after 13 days.

To illustrate this point, we performed a calculation with K_{zz} , decreased by a factor of 5 over the baseline profile (K_c), which is shown in Figures 8a–8d with the corresponding

decrease in water vapor abundance for each K_{zz} profile shown in Figure 9. The decrease in water vapor abundance above 80-km altitude essentially removes HO_x catalysis, resulting in a positive ozone response in that region. The calculated ozone response for this latter K_{zz} profile overlaps the error bars of the Keating *et al.* [1987] response.

Between about 70 and 80 km the calculated ozone response is out of phase with the solar UV forcing for both cases as shown in Figure 8c. This is a consequence of increased solar UV flux producing increased HO_x species. For the case of $K_{zz} = K_c$, with relatively high values of water vapor above 80 km, the out-of-phase relation continues above 80 km. For the case of K_{zz} decreased by a factor of 5 the ozone and solar flux start to become in phase between 80

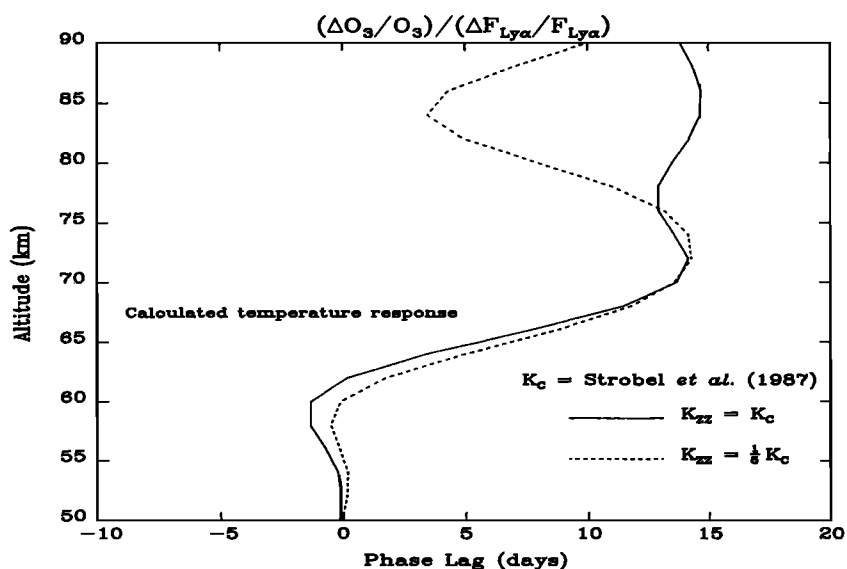


Fig. 8c. Ozone response phase lag.

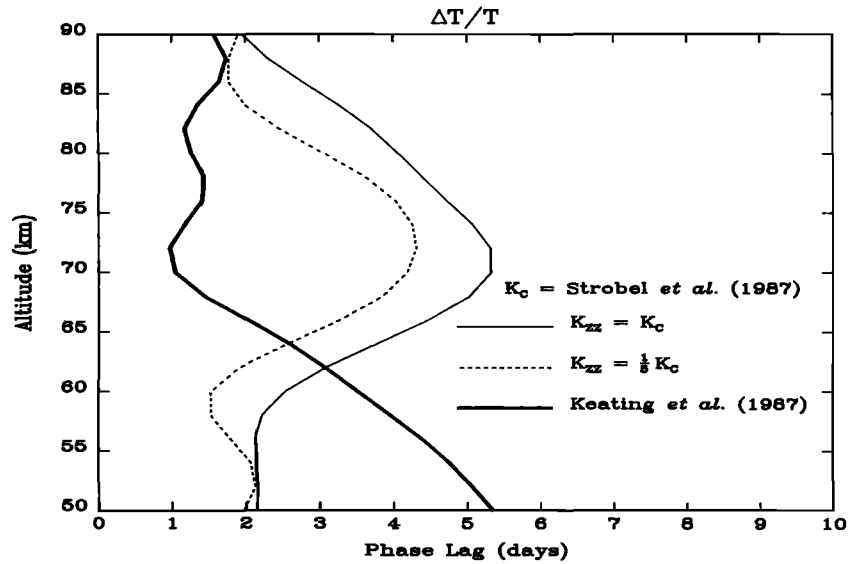


Fig. 8d. Temperature response phase lag for both cases, with the dark solid curve indicating the observed 2050-Å temperature phase response.

and 85 km, since HO_x chemistry plays no role in the ozone abundance. The decreasing role of HO_x chemistry is seen as a decreasing phase lag with decreasing altitude from 70 to 60 km. Below 60 km, photodissociation of water vapor is insignificant for ozone chemistry.

A positive ozone response implies positive local heating and, ignoring the radiative exchange between layers of the atmosphere, one expects a positive temperature response. The situation is complicated by the IR exchange. As shown in Figure 8b the temperature response is positive throughout the mesosphere but has a minimum near the maximum value of the negative ozone response. In the absence of radiative exchange the temperature response would be negative in that region. The fact that the temperature response is positive is indicative of the magnitude of IR radiative exchange. The phase lag (Figure 8d) between the temperature and solar flux is small where IR radiative exchange and HO_x chemistry

is unimportant but reaches a maximum value of near 5 days where these two effects peak in importance.

This model with low K_{zz} and the most rigorous treatment of the chemistry and physics of ozone variability predicts the essential aspects of the observed ozone response [Keating *et al.* 1987], in particular, the precise altitudes where the response reverses sign, for low K_{zz} . However, it is in almost complete disagreement with the observed temperature amplitude and phase lag. Given that the calculated ozone response is in essential agreement with the observed response, it is hard to understand how the observed temperature amplitude can have a large positive peak value at 70 km, precisely where the ozone perturbation heating has its maximum negative value (compare Figures 8a with 8b).

The calculated phase of the ozone response below 65 km is small (~1 day) but positive, in contrast to the calculated photochemical response by Hood and Douglass [1988], who

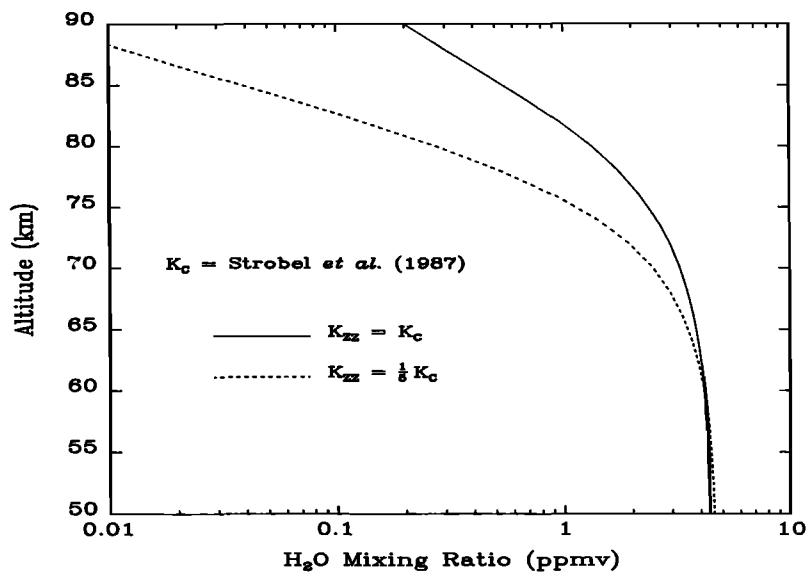


Fig. 9. Calculated water vapor mixing ratios for cases with baseline K_{zz} and baseline reduced by a factor of 5.

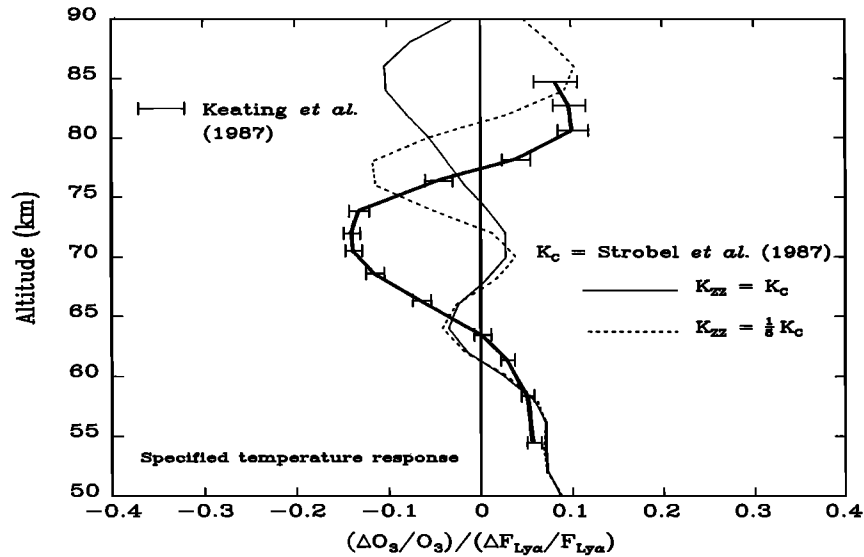


Fig. 10a. Ozone response for a sinusoidal variation of solar UV flux for model H, using the baseline model K_{zz} profile, and K_{zz} decreased by a factor of 5. Temperature response is prespecified, and temperature-chemistry feedback is included.

found large (~ 5 days) negative responses in the upper stratosphere when forced by observed temperature responses. The negative phase of the ozone response in their model is due to the fact that the observed temperature has a large (~ 5 day) positive phase lag relative to the solar UV forcing. The positive phase lag of the temperature in our model is of the order of 2 days, sufficiently small to eliminate the negative phase lag of ozone.

3.2.2. *Specified temperature response.* On the basis of a statistical study of Nimbus 7 Stratospheric and Mesospheric Sounder (SAMS) temperature data, Keating *et al.* [1987] deduced the temperature response to solar variability at 2050 Å. If the correlation between solar variability at Ly α and that at 2050 Å were large, then the calculated temperature response should mimic the observed response (above) if the theoretical description is accurate. The Keating *et al.*

[1987] temperature response (Figures 8b and 8d) is, in fact, substantially different from our calculated response. As a consistency check, we forced the temperature response amplitude and phase in the time-dependent model to match the Keating *et al.* [1987] temperature response, and then we calculated the time-dependent ozone response. The results, shown in Figures 10a and 10b, show marked disagreement with the ozone response deduced from SME data, especially in the region where the deduced temperature response maximizes (65 and 75 km) and generates a positive response. Lower eddy mixing improves the agreement with the SME ozone response curve above 75-km altitude, as in the case with the calculated temperature response, but does not change the positive response near 70-km altitude. The ~ 4 -day negative phase lag near 60-km altitude of the calculated ozone response with the prespecified temperature amplitude

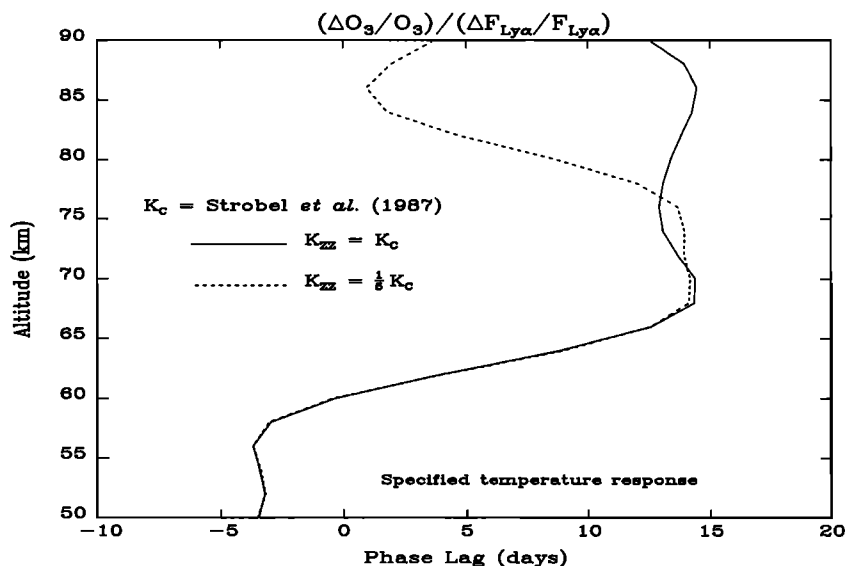


Fig. 10b. Ozone response phase lag.

and phase, as found by Hood and Douglass [1988], suggests that the observed temperature response to solar UV at 2050 Å is reliable. The solar flux at these long wavelengths is the driver of atmospheric temperature in the stratosphere. However, Ly α is the driver of HO_x in the mesosphere. On the basis of our examination of the SME UV flux data base, we found that the correlation of Ly α fluxes with those at 2000 Å and longward was generally not large. Thus the apparent disagreement near 60 km between calculations tied to Ly α variations and observations tied to 2050-Å flux variations is difficult to interpret. However, the disagreement between the calculated ozone response near 75 km and the observed response may suggest that there is a basic flaw in our understanding of HO_x chemistry in that region.

4. SUMMARY

Water vapor in the upper mesosphere exerts a strong influence on the magnitude of the observed ozone response to short-period solar UV flux variations. The water vapor abundance in the upper mesosphere is critically dependent on the magnitude of vertical transport in that region as demonstrated by Strobel *et al.* [1987]. The microwave measurements of Bevilacqua *et al.* [1989] indicate a dominant annual variation in upper mesospheric water vapor mixing ratios and by inference annual variations in vertical transport dominate. Hence we expect on the basis of our study that the water vapor seasonal variation produces a corresponding seasonal signature in the ozone response when the water vapor mixing ratio exceeds a threshold value, which we determined as ~ 1.5 ppmv at 80 km, a typical springtime value [Bevilacqua *et al.*, 1989]. This signature is of sufficient amplitude to mask other signatures in seasonally averaged ozone response data and necessitates organizing ozone data in the future according to common background water vapor concentrations in the upper mesosphere to extract these other signatures.

The ozone response in the lower mesosphere, below 70 km, reaches its asymptotic limiting value for enhanced solar ultraviolet flux on a time scale smaller than the solar rotation period, while the response above that region requires increasingly longer times to reach the asymptotic values. In the region near 80 km the ozone response after half a solar rotation period is only about 30% of its asymptotic value.

Finally, we note that the combined effects of water vapor variation, temperature-chemistry feedback effects, negligible solar flux variation longward of 2400 Å, and time-dependent nature of solar rotation driven ultraviolet flux forcing does reproduce the observed ozone response profile of Keating *et al.* [1987] from SME data, if eddy mixing rates were a factor of 5 smaller than recently inferred values [Strobel *et al.*, 1987]. It is unlikely, on the basis of our current water vapor data base which is restricted to essentially mid-latitudes in the northern hemisphere, that the actual upper mesospheric water vapor mixing ratios are an order of magnitude lower than inferred from observations [Bevilacqua *et al.*, 1989]. An alternative interpretation of our model results is that the HO_x catalytic removal of ozone is substantially less efficient than currently accepted photochemical reactions and rates imply and/or there is a fundamental flaw in our current understanding of HO_x reactions on ozone. The fact that the imposition of the Keating *et al.* [1987] deduced temperature amplitude and phase yields a

calculated ozone response to solar UV flux variations totally inconsistent with observations suggests the need for better mesospheric data and the use of solar UV spectral irradiance intervals that are highly correlated with mesospheric ozone and temperature variability. Last, additional observational and modeling efforts are required to determine whether dynamics plays a central role in the ozone and temperature response to solar UV variability.

Acknowledgments. The authors are indebted to D. E. Anderson, J. Rodriguez, and M. Nicolet for useful discussions and to W. J. Sawchuck for aid in developing the IDL graphics routines for producing several of the figures.

REFERENCES

- Aikin, A. C., and H. J. P. Smith, Mesospheric ozone changes associated with 27 day solar ultraviolet flux variations, *Geophys. Res. Lett.*, **13**, 427–430, 1986.
- Allen, M., Y. L. Yung, and J. M. Waters, Vertical transport and photochemistry in the terrestrial mesosphere and lower thermosphere (50–120 m), *J. Geophys. Res.*, **86**, 3617–3627, 1981.
- Allen, M., J. I. Lunine, and Y. L. Yung, The vertical distribution of ozone in the mesosphere and lower thermosphere, *J. Geophys. Res.*, **89**, 4841–4872, 1984.
- Barnett, J. J., and M. Corney, Middle atmosphere reference model derived from satellite data, in *Middle Atmosphere Program, Handbook for MAP*, vol. 16, pp. 47–85, ICSU Scientific Committee on Solar-Terrestrial Physics, Urbana, Ill., 1985.
- Bevilacqua, R. M., J. J. Olivero, P. R. Schwartz, C. J. Gibbins, J. M. Bologna, and D. L. Thacker, An observational study of water vapor in the mid-latitude mesosphere using ground-based microwave techniques, *J. Geophys. Res.*, **88**, 8523–8534, 1983.
- Bevilacqua, R. M., W. J. Wilson, W. B. Ricketts, P. R. Schwartz, and R. J. Howard, Possible seasonal variability of mesospheric water vapor, *Geophys. Res. Lett.*, **12**, 397–400, 1985.
- Bevilacqua, R. M., W. J. Wilson, and P. R. Schwartz, Measurements of mesospheric water vapor in 1984 and 1985: Results and implications for middle atmospheric transport, *J. Geophys. Res.*, **92**, 6679–6690, 1987.
- Bevilacqua, R. M., J. J. Olivero, and C. L. Croskey, Mesospheric water vapor measurements from Penn State: Observations and climatology, *J. Geophys. Res.*, **94**, 12,807–12,818, 1989.
- Bevilacqua, R. M., D. F. Strobel, M. E. Summers, J. J. Olivero, and M. Allen, The seasonal variation of water vapor and ozone in the upper mesosphere: Implications for vertical transport and ozone photochemistry, *J. Geophys. Res.*, **95**, 883–893, 1990.
- Brasseur, G., A. De Rudder, G. M. Keating, and M. C. Pitts, Response of middle atmosphere to short-term solar ultraviolet variations, 2, Theory, *J. Geophys. Res.*, **92**, 903–914, 1987.
- Chandra, S., The solar and dynamically induced oscillations in the stratosphere, *J. Geophys. Res.*, **91**, 2719–2734, 1986.
- Clancy, R. T., D. W. Rusch, R. J. Thomas, M. Allen, and R. S. Eckman, Model ozone photochemistry on the basis of Solar Mesosphere Explorer mesospheric observations, *J. Geophys. Res.*, **92**, 3067–3080, 1987.
- Cole, A. E., and A. J. Kantor, Air Force reference atmospheres, *AFGL Tech. Rep.*, AFGL-TR-78-0051, 1–89, 1978.
- Eckman, R. S., A theoretical and observational investigation of the response of ozone to short-term variations in the solar ultraviolet irradiance, Ph.D. thesis, Univ. of Colo., Boulder, 1985.
- Eckman, R. S., Response of ozone to short-term variations in the solar ultraviolet irradiance, 1, A theoretical model, *J. Geophys. Res.*, **91**, 6695–6704, 1986a.
- Eckman, R. S., Response of ozone to short-term variations in the solar ultraviolet irradiance, 2, Observations and interpretation, *J. Geophys. Res.*, **91**, 6705–6721, 1986b.
- Forbes, J. M., Thermosphere structure variations during high solar and magnetic activity conditions, final technical report, AF contract F19628-82-K0031, Boston Univ., Boston, Mass., 1985.
- Frederick, J. E., Chemical response of the middle atmosphere to changes in the ultraviolet solar flux, *Planet. Space Sci.*, **25**, 1–4, 1977.

- Garcia, R. R., S. Solomon, R. G. Roble, and D. W. Rusch, A numerical response of the middle atmosphere to the 11-year solar cycle, *Planet. Space Sci.*, 32, 411–423, 1984.
- Gille, J. C., C. M. Smythe, and D. F. Heath, Observed ozone response to variations in solar ultraviolet radiation, *Science*, 225, 315–317, 1984.
- Hood, L. L., Solar ultraviolet radiation-induced variations in the stratosphere and mesosphere, *J. Geophys. Res.*, 92, 876–888, 1987.
- Hood, L. L., and A. R. Douglass, Stratospheric responses to solar ultraviolet variations: Comparisons with photochemical models, *J. Geophys. Res.*, 93, 3905–3911, 1988.
- Keating, G. M., G. P. Brasseur, J. Y. Nicholson III, and A. De Rudder, Detection of the response of ozone in the middle atmosphere to short-term solar ultraviolet variations, *Geophys. Res. Lett.*, 12, 449–452, 1985.
- Keating, G. M., M. C. Pitts, G. Brasseur, and A. De Rudder, Response of middle atmosphere to short-term ultraviolet variations, 1, Observations, *J. Geophys. Res.*, 92, 889–902, 1987.
- Lean, J., Solar ultraviolet irradiance variations: A review, *J. Geophys. Res.*, 92, 839–868, 1987.
- Mohanakumar, M., An investigation on the influence of solar cycle on mesospheric temperature, *Planet. Space Sci.*, 33, 795–805, 1985.
- Rusch, D. W., and R. S. Eckman, Implications of the comparison of ozone abundances measured by the Solar Mesosphere Explorer to model calculations, *J. Geophys. Res.*, 90, 12,991–12,998, 1985.
- Strobel, D. F., Parameterization of the atmospheric heating rate from 15 to 120 km due to O₂ and O₃ absorption of solar radiation, *J. Geophys. Res.*, 83, 6225–6230, 1978.
- Strobel, D. F., M. E. Summers, R. M. Bevilacqua, M. T. DeLand, and M. Allen, Vertical constituent transport in the mesosphere, *J. Geophys. Res.*, 92, 6691–6698, 1987.
- Thomas, R. J., C. A. Barth, D. W. Rusch, and R. W. Sanders, Solar Mesosphere Explorer near-infrared spectrometer: Measurements of 1.27- μm radiances and the inference of mesospheric ozone, *J. Geophys. Res.*, 89, 9569–9580, 1984.
- Zhu, X., CO₂ 15 μm band cooling rates in the upper middle atmosphere calculated by Curtis matrix interpolation, *J. Atmos. Sci.*, 47, 755–774, 1990.
- Zhu, X., and D. F. Strobel, On the role of vibration-vibration transitions in radiative cooling of the CO₂ 15- μm band around the mesopause, *J. Geophys. Res.*, 95, 3571–3577, 1990a.
- Zhu, X., and D. F. Strobel, Radiative damping in the upper mesosphere, *J. Atmos. Sci.*, in press, 1990b.
-
- M. Allen, Earth and Space Sciences Division 183-601, Jet Propulsion Laboratory, 4800 Oak Grove Dr., Pasadena, CA 91109.
- R. M. Bevilacqua and M. E. Summers, E. O. Hulbert Center for Space Science, Naval Research Laboratory, Mail Code 4141.5, Washington, DC 20375.
- M. T. DeLand, ST Systems Corporation, 4400 Forbes Blvd., Lanham, MD 20706.
- G. M. Keating, Atmospheric Sciences Division, NASA Langley Research Center, Hampton, VA 23665.
- D. F. Strobel and X. Zhu, Department of Earth and Planetary Sciences, The Johns Hopkins University, Baltimore, MD 21218.

(Received August 10, 1989;
revised September 13, 1990;
accepted September 14, 1990.)